TECHNICAL REPORT

SPACE TELESCOPE SCIENCE INSTITUTE
Operated for NASA by AURA

Title: NIRCAM Optimal Readout II: General Case (Including Photon Noise)	Doc #: JWST-STScI-002100,SM-12 Date: 27 May 2010 Rev:
Authors: M. Robberto Phone: 410-338-4382	Release Date: 14 September 2010

1.0 Abstract

I calculate the signal-to-noise achieved with the NIRCam readout patterns as a function of the flux incident on a pixel. Out of the 110 possible combinations possible *a-priori*, 89 are "optimal", i.e. maximize the signal-to-noise ratio in a certain readout (or integration) time, for a given photon flux. I provide tables listing: a) the optimal readout pattern vs. integration time, for a wide range of photon fluxes (Table 3); b) the corresponding signal to noise (normalized to the value theoretically achievable for that flux using the longest readout pattern and in the absence of cosmic rays) and total (integrated) counts (Table 4); and c) a summary chart mapping the optimal readout pattern vs. readout time and photon flux (Table 6).

2.0 Introduction

The 9 NIRCam readout patterns (RAPID, BRIGHT1, BRIGHT2, SHALLOW2, SHALLOW4, MEDIUM2, MEDIUM8, DEEP2 and DEEP8), each made of either 10 or 20 groups, provide a total of 110 possible combinations corresponding to readout times ranging from 10.6s to 4112.8s. In Robberto (2009a, hereafter Paper 1) I have estimated the relative signal-to-noise ratio of each combination of readout pattern/number of groups in readout noise limited regime, finding that only 47 of them are "optimal", i.e. provide the highest signal-to-noise ratio for a given readout time, in the presence of cosmic rays. These combinations represent the optimal modes for NIRCAM operations in readout-noise-limited regime.

However, the noise terms due to the photon signal (both target and background) cannot, generally, be neglected. Table 1 reports the estimated background counts in 1000s integration, from the NIRCam Exposure Time Calculator (Rieke, 2005).

Table 1 Background flux in selected NIRCam Filters

Filter	Bkgnd Cts/pix/1000sec
F070W	143.41
F090W	165.50
F115W	179.74
F150W	169.30
F200W	165.89
F277W	574.08
F356W	384.54
F444W	1151.28

Assuming a readout noise of 15 electrons per sample ("single correlated"), the photon noise of these fluxes equals the readout noise variance at times ranging from 195s to 1570s. If one considers that several samples are averaged in groups, that the effective readout noise is further reduced by ramp fitting, and that Table 1 neglects the photon noise from the sources, it is clear that the detector can reach background limited conditions with relatively short integrations.

On the other hand, the table illustrates the case only for broad band filters (R~4). For medium band (R~10) and narrow-band (R~100) filters the flux scales down by factors of about 2.5 and 25, respectively, pushing up the crossing time between readout and background limited conditions. The bottom line is that photon flux cannot be ignored and one has to consider a broad range of illuminations.

In this report I provide a second set of tables describing how the effective readout noise varies with the readout pattern for different levels of the photon flux. The calculation follows the same analytic strategy adopted in Paper 1, with the exception that this time I use the full equation for the signal-to-noise, derived in Robberto (2009b, hereafter Paper 2).

3.0 Up-the-Ramp sampling: nomenclature

Before illustrating the results, I summarize the current nomenclature for the NIRCam readout modes.

NIRCam has 9 readout modes, each one composed by an integration, or ramp, sampled uniformly in time every t_f seconds. For full array readout, it is $t_f = 10.6$ seconds. Sets of adjacent frames can be either averaged into **groups** or ignored. The number of frames averaged into a group is given by m. If $m = 1$ the group is made by a single frame. Between groups there are s frames that are ignored, i.e. not saved in the spacecraft data recorder and transmitted to the ground. The time between adjacent groups is therefore given by $t_g = (m+s)t_f$. Any given combination of m and s defines a **readout pattern**. NIRCam has 110 readout patterns.

Table 2 summarizes the main parameters of the 9 NIRCAM readout modes. In this case it is m =2, s =3 and n =3. For a more complete description of the NIRCam readout patterns, see e.g. Section 4.2 "Multiaccum Readout Mode" of the NIRCAM Operation Concept Document (JWST-OPS-002843).

Table 2 Parameters of the 9 NIRCam readout patterns

Readout pattern	n^{max}	m	s
DEEP 8	20	8	12
DEEP2	20	2	18
MEDIUM8	10	8	2
MEDIUM2	10	2	8
SHALLOW4	10	4	1
SHALLOW2	10	2	3
BRIGHT2	10	2	1
BRIGHT1	10	1	1
RAPID	10	1	0

The ramp illustrated in Figure 1, adapted from Rauscher et al. (2007), illustrates the case in which $n = 6$, $m = 4$ and $s = 2$.

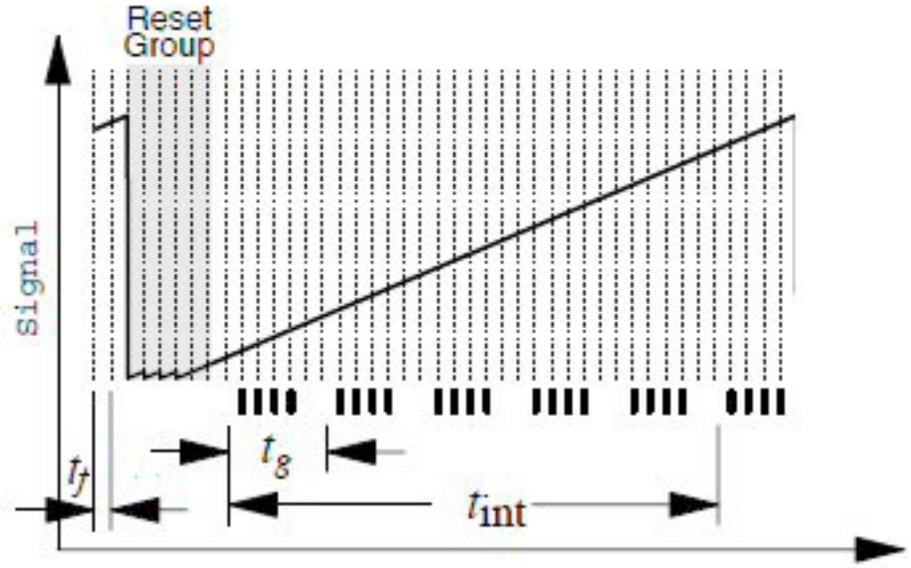

Figure 1 In MULTIACCUM mode, each pixel is reset and then non-destructively sampled many times during an integration, or ramp. Sampling occurs in 'groups', each composed by *n* samples sent to the Focal Plane Array Processor for coadding. Other *s* samples between groups are ignored. At the end, the detector is reset and returns in flush mode.

With these definitions, and indicating with b the flux in e/s/pix, the general equation describing the variance of the signal derived through line fitting of a readout pattern given in Paper 2 can be written in this form:

$$Var\left[S_{total}\right]=\frac{6}{5}\frac{\left(n^2+1\right)\left(n-1\right)}{n\left(n+1\right)}bt_g\left[1-\frac{5}{3}\frac{m^2-1}{m\left(n^2+1\right)}\frac{t_f}{t_g}\right]+12\frac{\left(n-1\right)}{n\left(n+1\right)}\frac{\sigma_{ron}{}^2}{m} \qquad (1)$$

4.0 Calculation

I have used the same method as in Paper 1, together with Equation (1) from Paper 2, assuming 6 different levels of photon flux per pixel. I started from the flux that equals the variance of the 15 electrons read noise, i.e. 225 electrons, in 3600s, i.e. 0.00625e/s/pix.

I have then multiplied this value by 1000, 100, 10, 1, 0.1 and 0.01 to covering the range of fluxes matching the 225e readout noise variance in 100 hours (basically the dark current, or the nearly ideal readout noise limited regime) to 3.6 seconds (high photon flux, completely background limited in the shortest exposure times). The calculation has been performed without and with cosmic rays, using the same parameters adopted in Paper 1 (i.e. 10 CR events per square cm per second), but only the results with cosmic rays are shown in this report. Let's just remember that cosmic rays may fall either within the *m* frames averaged in a group or between the *s* skipped frames. In both cases the ramp is broken in two parts, but in the first case the group has to be removed from further analysis, whereas in the second case both adjacent groups can be kept. The calculation statistically accounts for the location of cosmic rays within the integration and calculates a correction factor to the signal to noise ratio that does not depend on signal to noise ratio itself but only on the distribution of cosmic rays.

The set of Figures 2 to 7 shows the results obtained for the six levels of background/signal. Figure 2 is basically identical to Figure 3 of Paper 1, corresponding to the readout noise limited regime. The signal to noise grows in this case linearly with the integration time. A comparison of the other figures clearly show the progressive change of slope associated to entering the photon noise regime as signal accumulates. Eventually, for very high signals (Figure 7), the signal to noise increases from the very beginning with the square root of time, i.e. with a slope that is half the original slope (Figure 2) in our log-log plots.

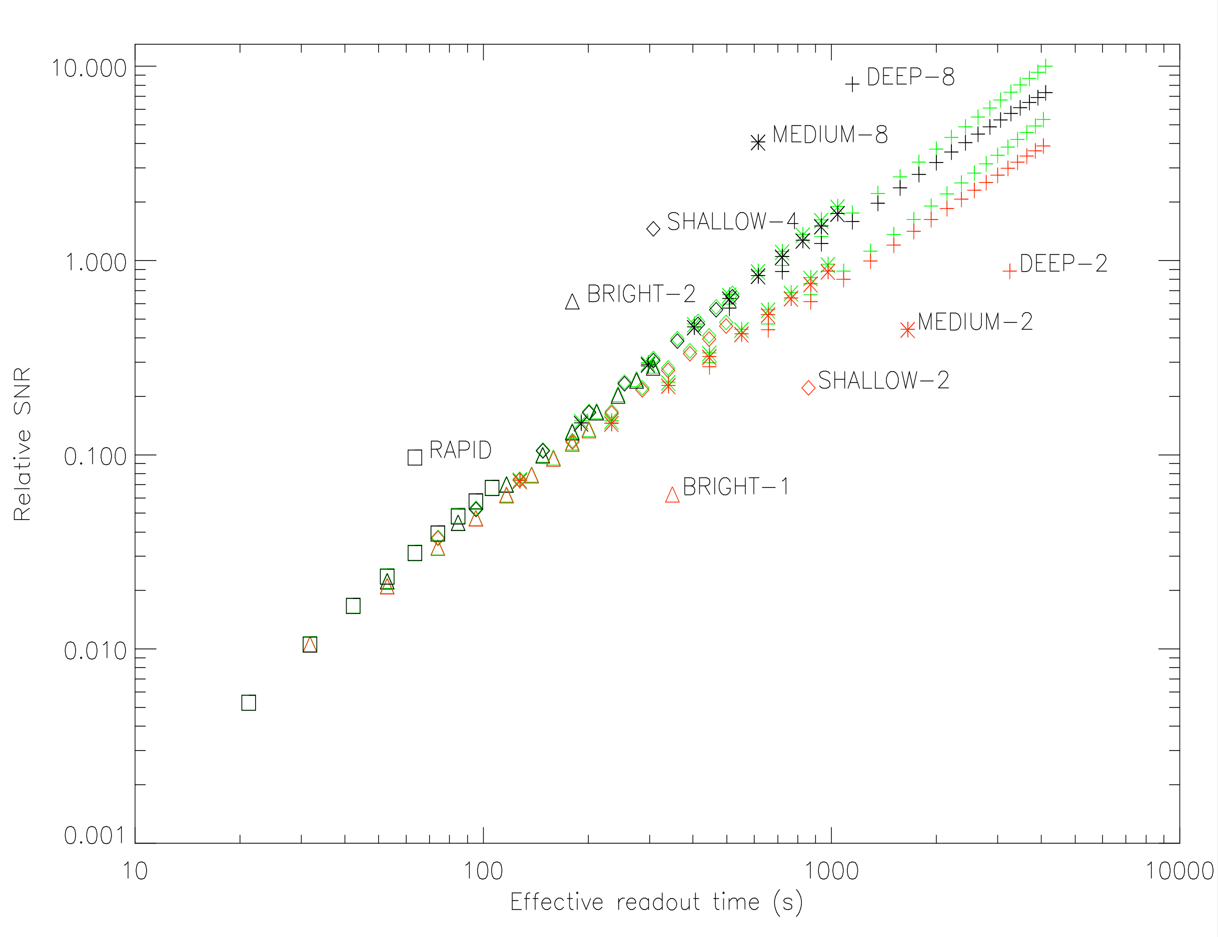

Figure 2 Signal-to-noise-ratio reached for the various NIRCam readout patterns with a signal that equalizes the readout noise variance in 100hr. Black and red symbols refer to readout patterns with small and large values of s, respectively, in the presence of cosmic rays. Green symbols represent the corresponding value in absence of cosmic ray.

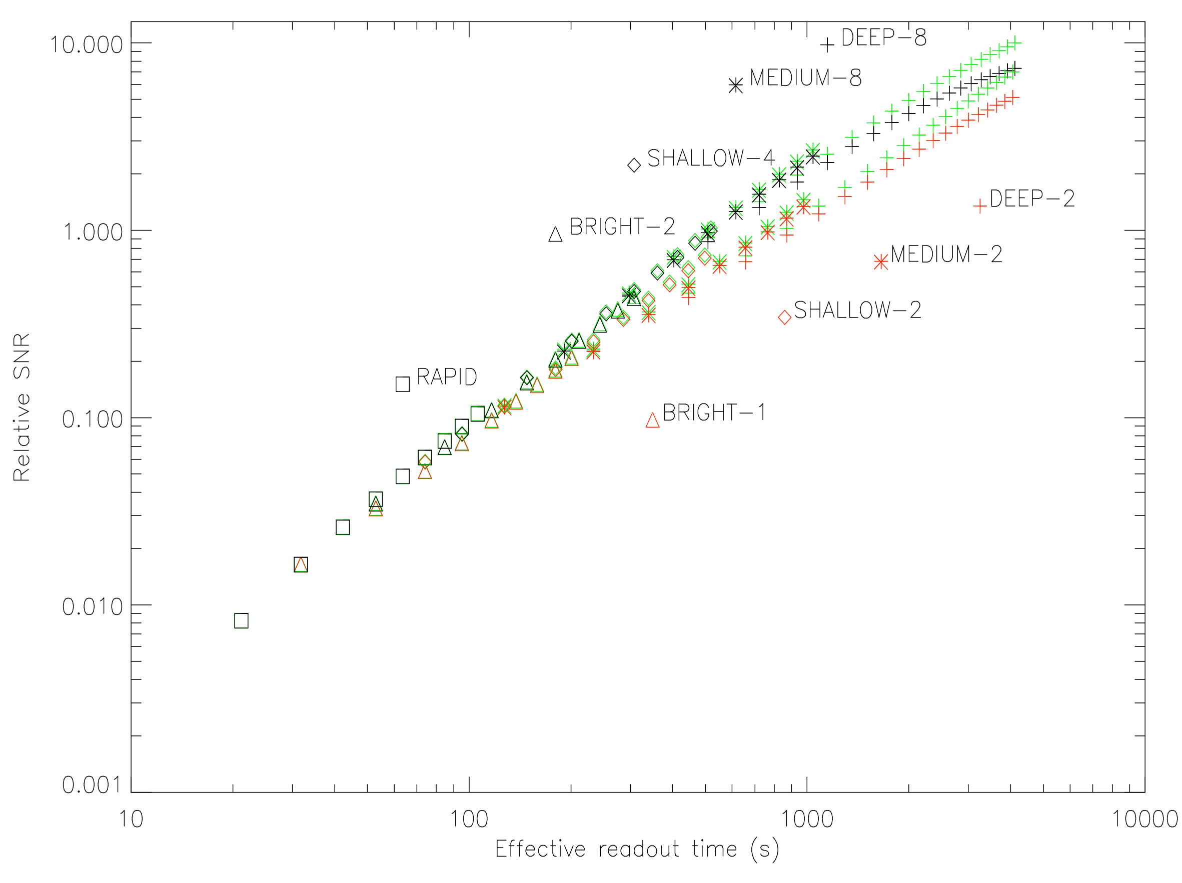

Figure 3 Signal-to-noise-ratio reached for the various NIRCam readout patterns with a signal that equalizes the readout noise variance in 10 hr. Same symbols as Figure 2.

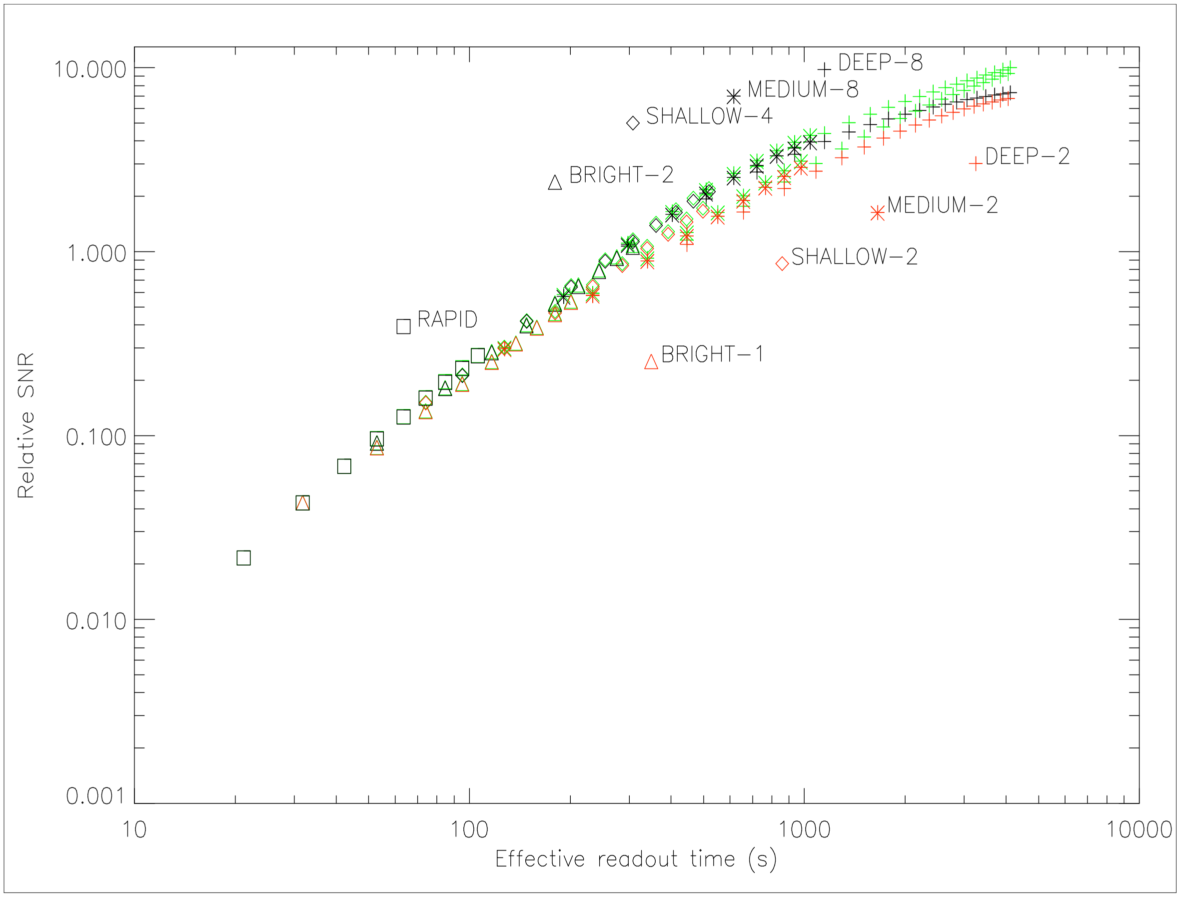

Figure 4 Signal-to-noise-ratio reached for the various NIRCam readout patterns with a signal that equalizes the readout noise variance in 1 hr. Same symbols as Figure 2.

Figure 5 Signal-to-noise-ratio reached for the various NIRCam readout patterns with a signal that equalizes the readout noise variance in 6 min. Same symbols as Figure 2.

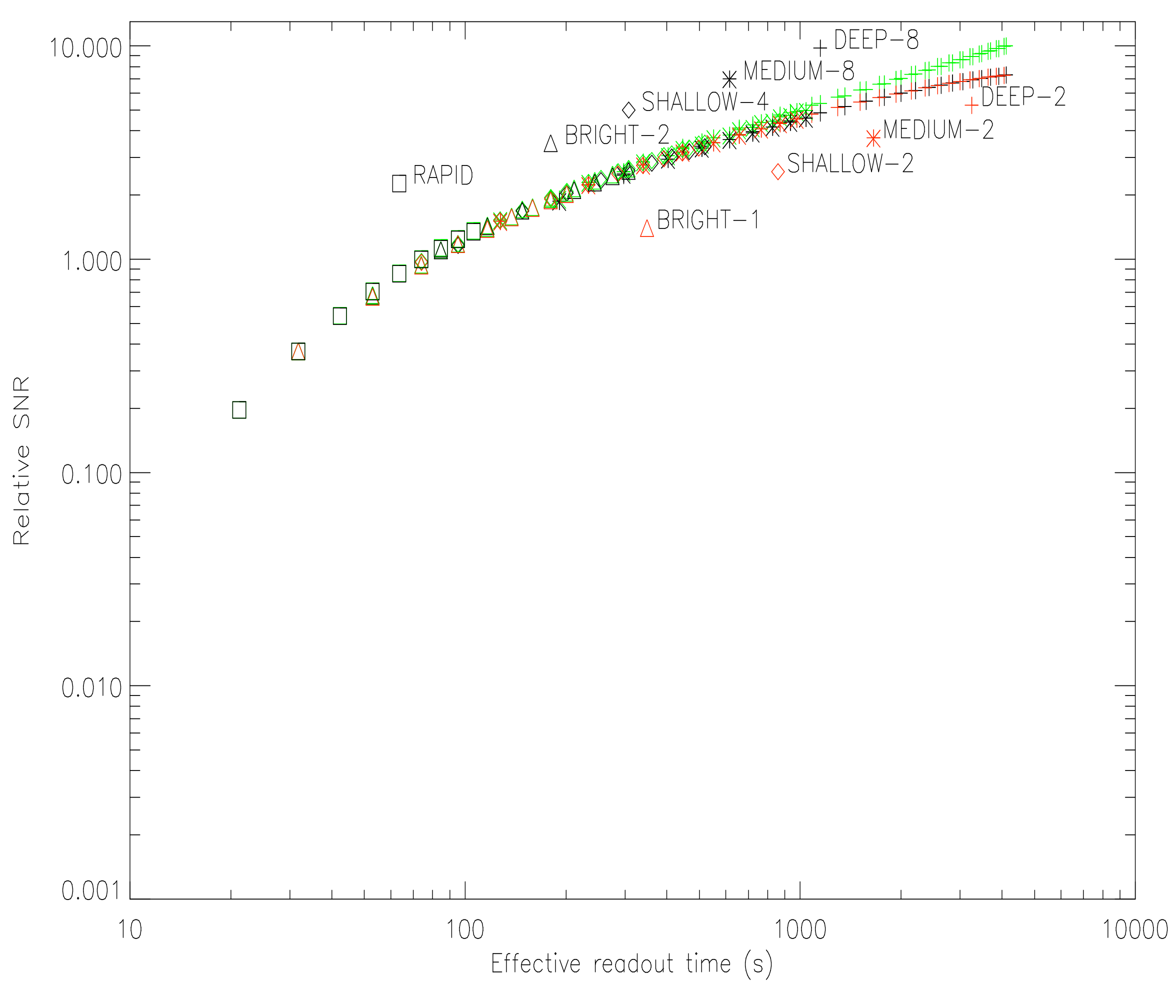

Figure 6 Signal-to-noise-ratio reached for the various NIRCam readout patterns with a signal that equalizes the readout noise variance in 36 s. Same symbols as Figure 2.

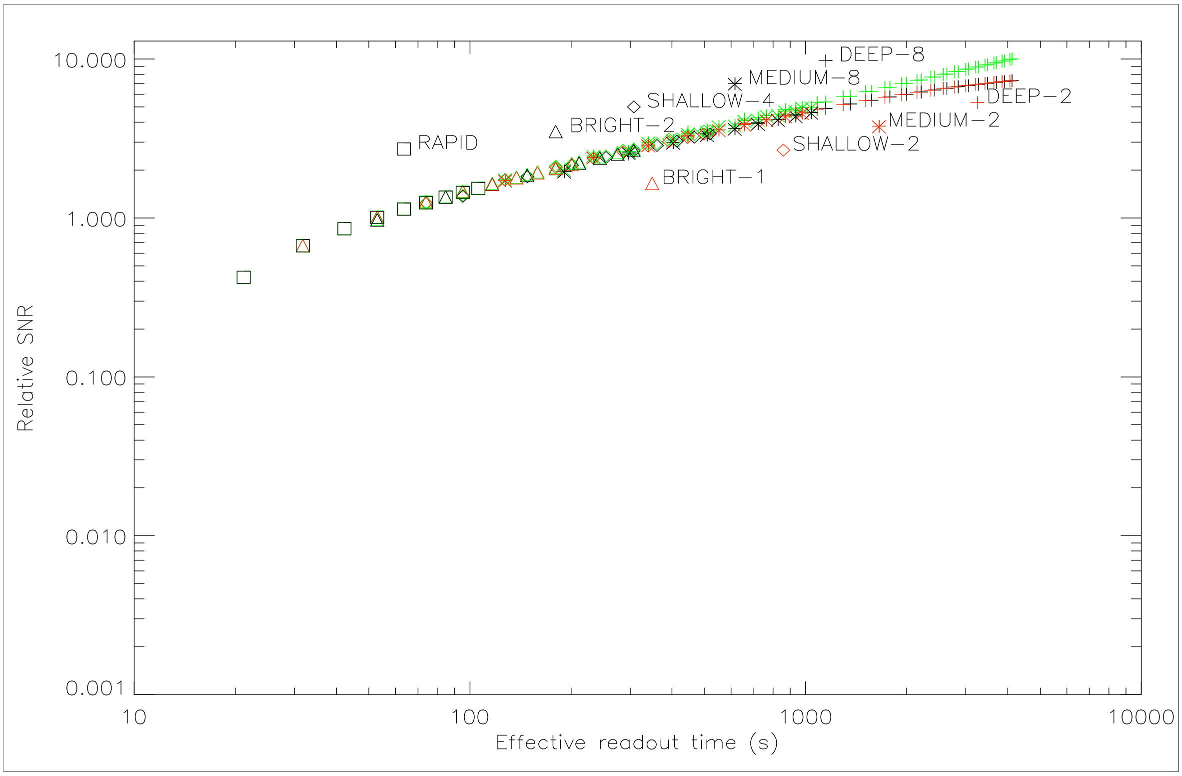

Figure 7 Signal-to-noise-ratio reached for the various NIRCam readout patterns with a signal that equalizes the readout noise variance in 3.6s. Same symbols as Figure 2.

5.0 Results

The 110 NIRCam readout patterns correspond to 75 exposure times, shown in the leftmost column of Table 3. I do not include the 10.6 exposure time, which can be achieved in two modes (BRIGHT1 and RAPID) setting n=1: with only one read no fit is possible and Equation (1) cannot be applied. The remaining 33 exposure times are degenerate, i.e. they can be reached in more than one readout pattern. This degeneracy is removed in Table 3 which reports, for the 75 unique exposure times, the readout pattern that provide2 the highest signal to noise for each signal level, from very low (readout noise limited regime, column 2) to high (photon noise limited regime, column 7). Column 1 is basically coincident with the "pure readout noise limited case" treated in Paper 1.

Table 3 clearly shows that for any given integration time the best readout pattern depends on the photon flux. For example, the 233.2 s case has three possible solutions: for the 0.000625e/s/pix photon flux the best readout pattern is DEEP2-2; for the 0.00625e/s/pix photon flux the best readout pattern is MEDIUM2-3; for the 0.0625e/s/pix photon flux, and higher, the best readout pattern is SHALLOW2-5.

If we consider the actual values of the signal to noise ratios obtained with these readout patterns (Table 4), we see that for certain times (yellow boxes) the best readout pattern provides a signal to noise *lower* than the signal to noise achieved with an immediately shorter integration time. This because the signal to noise depends not only on the photon flux but also on the number of reads which are averaged in a group (as discussed in Paper 1). These readout patterns should not therefore be considered as “optimal”. One may notice that the DEEP2-2, MEDIUM2-3 and one of the SHALLOW2-5 patterns found in the 233.2s case (Table 3) fall in this category.

For convenience, I report in Table 5 the integrated counts at the end of each exposure. For each exposure time they scale, as expected, by a factor of 10 across columns. One may notice that the leftmost column can be regarded as representative of the detector dark current, whereas for integration times longer than ~1700s the rightmost column returns counts higher than 100,000. We can use this value as a saturation flag, and mark accordingly the cell background in red color.

Finally, Table 6 summarizes the result with a map of the optimal readout patterns to be used for a given exposure time, at the flux levels we have considered. Only optimal readout patterns have been considered, and the red color still indicates readout patterns that would correspond to pixel saturation.

Table 3 Best readout patterns for each exposure time versus photon rate

	0.000625e/s		**0.00625e/s**		**0.0625e/s**		**0.625e/s**		**6.25e/s**		**62.5e/s**	
IT	**RAMP**	**n**	**RAMP**	**n**	**RAMP**	**n**	**RAMP**	**n**	**RAMP**	**n**	**RAMP**	**n**
21.2	RAPID	2	RAPID	2	RAPID	2	RAPID	2	RAPID	2	RAPID	2
31.8	RAPID	3	RAPID	3	RAPID	3	RAPID	3	RAPID	3	RAPID	3
42.4	RAPID	4	RAPID	4	RAPID	4	RAPID	4	RAPID	4	RAPID	4
53	BRIGHT1	3	RAPID	5	RAPID	5	RAPID	5	RAPID	5	RAPID	5
63.6	RAPID	6	RAPID	6	RAPID	6	RAPID	6	RAPID	6	RAPID	6
74.2	BRIGHT1	4	RAPID	7	RAPID	7	RAPID	7	RAPID	7	RAPID	7
84.8	BRIGH2	3	RAPID	8	RAPID	8	RAPID	8	RAPID	8	RAPID	8
95.4	BRIGHT1	5	RAPID	9	RAPID	9	RAPID	9	RAPID	9	RAPID	9
106	RAPID	10	RAPID	10	RAPID	10	RAPID	10	RAPID	10	RAPID	10
116.6	BRIGHT1	6	BRIGH2	4	BRIGH2	4	BRIGH2	4	BRIGH2	4	BRIGH2	4
127.2	MEDIUM2	2	SHALLOW2	3	SHALLOW2	3	SHALLOW2	3	SHALLOW2	3	SHALLOW2	3
137.8	BRIGHT1	7	BRIGHT1	7	BRIGHT1	7	BRIGHT1	7	BRIGHT1	7	BRIGHT1	7
148.4	BRIGH2	5	BRIGH2	5	SHALLOW4	3	SHALLOW4	3	SHALLOW4	3	SHALLOW4	3
159	BRIGHT1	8	BRIGHT1	8	BRIGHT1	8	BRIGHT1	8	BRIGHT1	8	BRIGHT1	8
180.2	SHALLOW2	4	SHALLOW2	4	BRIGH2	6	BRIGH2	6	BRIGH2	6	BRIGH2	6
190.8	MEDIUM8	2	MEDIUM8	2	MEDIUM8	2	MEDIUM8	2	MEDIUM8	2	MEDIUM8	2
201.4	BRIGHT1	10	SHALLOW4	4	SHALLOW4	4	SHALLOW4	4	SHALLOW4	4	SHALLOW4	4
212	BRIGH2	7	BRIGH2	7	BRIGH2	7	BRIGH2	7	BRIGH2	7	BRIGH2	7
233.2	DEEP2	2	MEDIUM2	3	SHALLOW2	5	SHALLOW2	5	SHALLOW2	5	SHALLOW2	5
243.8	BRIGH2	8	BRIGH2	8	BRIGH2	8	BRIGH2	8	BRIGH2	8	BRIGH2	8
254.4	SHALLOW4	5	SHALLOW4	5	SHALLOW4	5	SHALLOW4	5	SHALLOW4	5	SHALLOW4	5
275.6	BRIGH2	9	BRIGH2	9	BRIGH2	9	BRIGH2	9	BRIGH2	9	BRIGH2	9
286.2	SHALLOW2	6	SHALLOW2	6	SHALLOW2	6	SHALLOW2	6	SHALLOW2	6	SHALLOW2	6

	0.000625e/s		**0.00625e/s**		**0.0625e/s**		**0.625e/s**		**6.25e/s**		**62.5e/s**	
IT	**RAMP**	**n**	**RAMP**	**n**	**RAMP**	**n**	**RAMP**	**n**	**RAMP**	**n**	**RAMP**	**n**
296.8	DEEP8	2	MEDIUM8	3	MEDIUM8	3	MEDIUM8	3	MEDIUM8	3	MEDIUM8	3
307.4	BRIGH2	10	BRIGH2	10	SHALLOW4	6	SHALLOW4	6	SHALLOW4	6	SHALLOW4	6
339.2	MEDIUM2	4	MEDIUM2	4	SHALLOW2	7	SHALLOW2	7	SHALLOW2	7	SHALLOW2	7
360.4	SHALLOW4	7	SHALLOW4	7	SHALLOW4	7	SHALLOW4	7	SHALLOW4	7	SHALLOW4	7
392.2	SHALLOW2	8	SHALLOW2	8	SHALLOW2	8	SHALLOW2	8	SHALLOW2	8	SHALLOW2	8
402.8	MEDIUM8	4	MEDIUM8	4	MEDIUM8	4	MEDIUM8	4	MEDIUM8	4	MEDIUM8	4
413.4	SHALLOW4	8	SHALLOW4	8	SHALLOW4	8	SHALLOW4	8	SHALLOW4	8	SHALLOW4	8
445.2	DEEP2	3	DEEP2	3	SHALLOW2	9	SHALLOW2	9	SHALLOW2	9	SHALLOW2	9
466.4	SHALLOW4	9	SHALLOW4	9	SHALLOW4	9	SHALLOW4	9	SHALLOW4	9	SHALLOW4	9
498.2	SHALLOW2	10	SHALLOW2	10	SHALLOW2	10	SHALLOW2	10	SHALLOW2	10	SHALLOW2	10
508.8	DEEP8	3	DEEP8	3	DEEP8	3	MEDIUM8	5	MEDIUM8	5	MEDIUM8	5
519.4	SHALLOW4	10	SHALLOW4	10	SHALLOW4	10	SHALLOW4	10	SHALLOW4	10	SHALLOW4	10
551.2	MEDIUM2	6	MEDIUM2	6	MEDIUM2	6	MEDIUM2	6	MEDIUM2	6	MEDIUM2	6
614.8	MEDIUM8	6	MEDIUM8	6	MEDIUM8	6	MEDIUM8	6	MEDIUM8	6	MEDIUM8	6
657.2	DEEP2	4	DEEP2	4	MEDIUM2	7	MEDIUM2	7	MEDIUM2	7	MEDIUM2	7
720.8	DEEP8	4	DEEP8	4	DEEP8	4	MEDIUM8	7	MEDIUM8	7	MEDIUM8	7
763.2	MEDIUM2	8	MEDIUM2	8	MEDIUM2	8	MEDIUM2	8	MEDIUM2	8	MEDIUM2	8
826.8	MEDIUM8	8	MEDIUM8	8	MEDIUM8	8	MEDIUM8	8	MEDIUM8	8	MEDIUM8	8
869.2	DEEP2	5	DEEP2	5	MEDIUM2	9	MEDIUM2	9	MEDIUM2	9	MEDIUM2	9
932.8	DEEP8	5	DEEP8	5	DEEP8	5	MEDIUM8	9	MEDIUM8	9	MEDIUM8	9
975.2	MEDIUM2	10	MEDIUM2	10	MEDIUM2	10	MEDIUM2	10	MEDIUM2	10	MEDIUM2	10
1038.8	MEDIUM8	10	MEDIUM8	10	MEDIUM8	10	MEDIUM8	10	MEDIUM8	10	MEDIUM8	10
1081.2	DEEP2	6	DEEP2	6	DEEP2	6	DEEP2	6	DEEP2	6	DEEP2	6
1144.8	DEEP8	6	DEEP8	6	DEEP8	6	DEEP8	6	DEEP8	6	DEEP8	6

	0.000625e/s		**0.00625e/s**		**0.0625e/s**		**0.625e/s**		**6.25e/s**		**62.5e/s**	
IT	**RAMP**	**n**	**RAMP**	**n**	**RAMP**	**n**	**RAMP**	**n**	**RAMP**	**n**	**RAMP**	**n**
1293.2	DEEP2	7	DEEP2	7	DEEP2	7	DEEP2	7	DEEP2	7	DEEP2	7
1356.8	DEEP8	7	DEEP8	7	DEEP8	7	DEEP8	7	DEEP8	7	DEEP8	7
1505.2	DEEP2	8	DEEP2	8	DEEP2	8	DEEP2	8	DEEP2	8	DEEP2	8
1568.8	DEEP8	8	DEEP8	8	DEEP8	8	DEEP8	8	DEEP8	8	DEEP8	8
1717.2	DEEP2	9	DEEP2	9	DEEP2	9	DEEP2	9	DEEP2	9	DEEP2	9
1780.8	DEEP8	9	DEEP8	9	DEEP8	9	DEEP8	9	DEEP8	9	DEEP8	9
1929.2	DEEP2	10	DEEP2	10	DEEP2	10	DEEP2	10	DEEP2	10	DEEP2	10
1992.8	DEEP8	10	DEEP8	10	DEEP8	10	DEEP8	10	DEEP8	10	DEEP8	10
2141.2	DEEP2	11	DEEP2	11	DEEP2	11	DEEP2	11	DEEP2	11	DEEP2	11
2204.8	DEEP8	11	DEEP8	11	DEEP8	11	DEEP8	11	DEEP8	11	DEEP8	11
2353.2	DEEP2	12	DEEP2	12	DEEP2	12	DEEP2	12	DEEP2	12	DEEP2	12
2416.8	DEEP8	12	DEEP8	12	DEEP8	12	DEEP8	12	DEEP8	12	DEEP8	12
2565.2	DEEP2	13	DEEP2	13	DEEP2	13	DEEP2	13	DEEP2	13	DEEP2	13
2628.8	DEEP8	13	DEEP8	13	DEEP8	13	DEEP8	13	DEEP8	13	DEEP8	13
2777.2	DEEP2	14	DEEP2	14	DEEP2	14	DEEP2	14	DEEP2	14	DEEP2	14
2840.8	DEEP8	14	DEEP8	14	DEEP8	14	DEEP8	14	DEEP8	14	DEEP8	14
2989.2	DEEP2	15	DEEP2	15	DEEP2	15	DEEP2	15	DEEP2	15	DEEP2	15
3052.8	DEEP8	15	DEEP8	15	DEEP8	15	DEEP8	15	DEEP8	15	DEEP8	15
3201.2	DEEP2	16	DEEP2	16	DEEP2	16	DEEP2	16	DEEP2	16	DEEP2	16
3264.8	DEEP8	16	DEEP8	16	DEEP8	16	DEEP8	16	DEEP8	16	DEEP8	16
3413.2	DEEP2	17	DEEP2	17	DEEP2	17	DEEP2	17	DEEP2	17	DEEP2	17
3476.8	DEEP8	17	DEEP8	17	DEEP8	17	DEEP8	17	DEEP8	17	DEEP8	17
3625.2	DEEP2	18	DEEP2	18	DEEP2	18	DEEP2	18	DEEP2	18	DEEP2	18
3688.8	DEEP8	18	DEEP8	18	DEEP8	18	DEEP8	18	DEEP8	18	DEEP8	18

	0.000625e/s		**0.00625e/s**		**0.0625e/s**		**0.625e/s**		**6.25e/s**		**62.5e/s**	
IT	**RAMP**	**n**	**RAMP**	**n**	**RAMP**	**n**	**RAMP**	**n**	**RAMP**	**n**	**RAMP**	**n**
3837.2	DEEP2	19	DEEP2	19	DEEP2	19	DEEP2	19	DEEP2	19	DEEP2	19
3900.8	DEEP8	19	DEEP8	19	DEEP8	19	DEEP8	19	DEEP8	19	DEEP8	19
4049.2	DEEP2	20	DEEP2	20	DEEP2	20	DEEP2	20	DEEP2	20	DEEP2	20
4112.8	DEEP8	20	DEEP8	20	DEEP8	20	DEEP8	20	DEEP8	20	DEEP8	20

Table 4 Signal to noise corresponding to the readout patterns of Table 3, normalized to the maximum signal to noise which would be achieved with the DEEP8-20 mode without cosmic ray. The yellow cells represent non-optimal combinations of readout pattern and number of groups.

	SNR/SNR(max)					
IT (s)	**0.000625e/s**	**0.00625e/s**	**0.0625e/s**	**0.625e/s**	**6.25e/s**	**62.5e/s**
21.2	0.00053	0.00082	0.00216	0.00662	0.01963	0.04228
31.8	0.00105	0.00164	0.0043	0.01312	0.03691	0.06685
42.4	0.00167	0.00259	0.00679	0.02053	0.05417	0.0856
53	0.00235	0.00367	0.00958	0.02865	0.07057	0.1009
63.6	0.00311	0.00484	0.01265	0.03731	0.08575	0.11363
74.2	0.00393	0.00612	0.01596	0.04636	0.09964	0.126
84.8	0.00481	0.00749	0.01948	0.05568	0.11232	0.13529
95.4	0.00575	0.00894	0.02321	0.06514	0.12392	0.14619
106	0.00673	0.01048	0.02712	0.07466	0.13458	0.15299
116.6	0.00701	0.01091	0.02827	0.07813	0.14232	0.16336
127.2	0.00738	0.01149	0.02976	0.08242	0.15094	0.17205
137.8	0.00782	0.01217	0.0315	0.0868	0.15686	0.17851
148.4	0.01045	0.01625	0.04167	0.10726	0.169	0.18493
159	0.00956	0.01487	0.03835	0.10269	0.17338	0.19218
180.2	0.01306	0.02029	0.05178	0.1289	0.19111	0.20768
190.8	0.01458	0.02263	0.05718	0.13474	0.1867	0.19598
201.4	0.0164	0.02545	0.06417	0.1493	0.204	0.21637
212	0.01648	0.02558	0.06465	0.15235	0.2111	0.2216
233.2	0.01635	0.0254	0.06449	0.15615	0.22349	0.23904
243.8	0.02014	0.03122	0.07805	0.17422	0.22857	0.23734
254.4	0.02311	0.03578	0.08832	0.18634	0.23351	0.2405
275.6	0.02401	0.03717	0.09184	0.1945	0.24442	0.25187
286.2	0.02155	0.03342	0.08375	0.18906	0.25065	0.26078
296.8	0.02921	0.04511	0.10891	0.2116	0.25149	0.25275
307.4	0.03045	0.04701	0.11326	0.21851	0.259	0.26541
339.2	0.02715	0.04203	0.10375	0.21889	0.27585	0.28797
360.4	0.03836	0.05902	0.13842	0.24662	0.28084	0.28513
392.2	0.03312	0.05117	0.12421	0.24587	0.29538	0.3022
402.8	0.0455	0.06975	0.15922	0.2657	0.29483	0.29832
413.4	0.04678	0.0717	0.16337	0.27151	0.30083	0.30433
445.2	0.03942	0.06077	0.14487	0.27033	0.31786	0.32975
466.4	0.05567	0.08496	0.1878	0.29381	0.31912	0.32204
498.2	0.04603	0.07079	0.16552	0.29259	0.33207	0.33698
508.8	0.06384	0.09699	0.20811	0.30926	0.33796	0.3413
519.4	0.06499	0.09872	0.21148	0.31401	0.33603	0.33851

	SNR/SNR(max)					
IT (s)	**0.000625e/s**	**0.00625e/s**	**0.0625e/s**	**0.625e/s**	**6.25e/s**	**62.5e/s**
551.2	0.04203	0.06486	0.15593	0.29872	0.35229	0.35943
614.8	0.08374	0.12586	0.25337	0.34631	0.36331	0.36516
657.2	0.05274	0.08112	0.18986	0.33649	0.38458	0.39305
720.8	0.10498	0.15583	0.29456	0.37725	0.39748	0.39969
763.2	0.06407	0.09817	0.22325	0.36954	0.40886	0.41355
826.8	0.12739	0.18648	0.33178	0.40521	0.41611	0.41726
869.2	0.07595	0.11587	0.25568	0.39877	0.43667	0.44294
932.8	0.1508	0.21744	0.36536	0.43135	0.44612	0.44769
975.2	0.08832	0.13411	0.28686	0.42491	0.45442	0.45774
1038.8	0.17509	0.24839	0.3957	0.45215	0.4596	0.46037
1081.2	0.07997	0.12225	0.27354	0.4379	0.47907	0.48388
1144.8	0.15883	0.23064	0.39759	0.47525	0.48635	0.48751
1293.2	0.09957	0.15123	0.32399	0.48106	0.5148	0.5186
1356.8	0.19735	0.28021	0.44754	0.51205	0.52059	0.52147
1505.2	0.12001	0.18094	0.37076	0.51762	0.54558	0.54865
1568.8	0.23728	0.32877	0.49035	0.54362	0.5503	0.55098
1717.2	0.14114	0.21104	0.41361	0.54903	0.57246	0.57499
1780.8	0.27827	0.37568	0.52727	0.57111	0.57638	0.57692
1929.2	0.16281	0.24127	0.45257	0.57633	0.59617	0.59828
1992.8	0.31999	0.42047	0.55933	0.59528	0.59948	0.59991
2141.2	0.18491	0.27137	0.4878	0.60027	0.61721	0.61899
2204.8	0.36218	0.46287	0.58736	0.6167	0.62005	0.62039
2353.2	0.20735	0.30116	0.51959	0.62142	0.63599	0.63751
2416.8	0.40461	0.50269	0.612	0.63577	0.63844	0.63871
2565.2	0.23002	0.33044	0.54818	0.64015	0.65276	0.65407
2628.8	0.44705	0.53987	0.63375	0.65281	0.65491	0.65513
2777.2	0.25284	0.35906	0.57387	0.6568	0.66778	0.66891
2840.8	0.48931	0.5744	0.653	0.66803	0.66968	0.66984
2989.2	0.27575	0.38692	0.59694	0.67164	0.68124	0.68223
3052.8	0.53122	0.60634	0.67009	0.68167	0.68292	0.68305
3201.2	0.29866	0.41389	0.61762	0.68486	0.69329	0.69415
3264.8	0.57263	0.63577	0.68527	0.69387	0.69479	0.69488
3413.2	0.32153	0.43991	0.63616	0.69664	0.70406	0.70482
3476.8	0.6134	0.6628	0.69876	0.70476	0.70541	0.70547
3625.2	0.34428	0.46488	0.65273	0.70709	0.71364	0.71431
3688.8	0.6534	0.68754	0.71073	0.71447	0.71486	0.7149
3837.2	0.36689	0.48881	0.66756	0.7164	0.72219	0.72278

	SNR/SNR(max)					
IT (s)	**0.000625e/s**	**0.00625e/s**	**0.0625e/s**	**0.625e/s**	**6.25e/s**	**62.5e/s**
3900.8	0.69254	0.71015	0.72134	0.7231	0.72328	0.7233
4049.2	0.38928	0.51161	0.68077	0.7246	0.72972	0.73024
4112.8	0.73072	0.73072	0.73072	0.73072	0.73072	0.73072

Table 5 Integrated counts vs. integration time and photon flux. Red cells indicate saturation.

	Integrated counts					
IT (s)	***0.000625e/s***	***0.00625e/s***	***0.0625e/s***	***0.625e/s***	***6.25e/s***	***62.5e/s***
21.2	0.01325	0.1325	1.325	13.25	132.5	1325
31.8	0.019875	0.19875	1.9875	19.875	198.75	1987.5
42.4	0.0265	0.265	2.65	26.5	265	2650
53	0.033125	0.33125	3.3125	33.125	331.25	3312.5
63.6	0.03975	0.3975	3.975	39.75	397.5	3975
74.2	0.046375	0.46375	4.6375	46.375	463.75	4637.5
84.8	0.053	0.53	5.3	53	530	5300
95.4	0.059625	0.59625	5.9625	59.625	596.25	5962.5
106	0.06625	0.6625	6.625	66.25	662.5	6625
116.6	0.072875	0.72875	7.2875	72.875	728.75	7287.5
127.2	0.0795	0.795	7.95	79.5	795	7950
137.8	0.086125	0.86125	8.6125	86.125	861.25	8612.5
148.4	0.09275	0.9275	9.275	92.75	927.5	9275
159	0.099375	0.99375	9.9375	99.375	993.75	9937.5
180.2	0.112625	1.12625	11.2625	112.625	1126.25	11262.5
190.8	0.11925	1.1925	11.925	119.25	1192.5	11925
201.4	0.125875	1.25875	12.5875	125.875	1258.75	12587.5
212	0.1325	1.325	13.25	132.5	1325	13250
233.2	0.14575	1.4575	14.575	145.75	1457.5	14575
243.8	0.152375	1.52375	15.2375	152.375	1523.75	15237.5
254.4	0.159	1.59	15.9	159	1590	15900
275.6	0.17225	1.7225	17.225	172.25	1722.5	17225
286.2	0.178875	1.78875	17.8875	178.875	1788.75	17887.5
296.8	0.1855	1.855	18.55	185.5	1855	18550
307.4	0.192125	1.92125	19.2125	192.125	1921.25	19212.5
339.2	0.212	2.12	21.2	212	2120	21200
360.4	0.22525	2.2525	22.525	225.25	2252.5	22525
392.2	0.245125	2.45125	24.5125	245.125	2451.25	24512.5
402.8	0.25175	2.5175	25.175	251.75	2517.5	25175
413.4	0.258375	2.58375	25.8375	258.375	2583.75	25837.5

	Integrated counts					
IT (s)	***0.000625e/s***	***0.00625e/s***	***0.0625e/s***	***0.625e/s***	***6.25e/s***	***62.5e/s***
445.2	0.27825	2.7825	27.825	278.25	2782.5	27825
466.4	0.2915	2.915	29.15	291.5	2915	29150
498.2	0.311375	3.11375	31.1375	311.375	3113.75	31137.5
508.8	0.318	3.18	31.8	318	3180	31800
519.4	0.324625	3.24625	32.4625	324.625	3246.25	32462.5
551.2	0.3445	3.445	34.45	344.5	3445	34450
614.8	0.38425	3.8425	38.425	384.25	3842.5	38425
657.2	0.41075	4.1075	41.075	410.75	4107.5	41075
720.8	0.4505	4.505	45.05	450.5	4505	45050
763.2	0.477	4.77	47.7	477	4770	47700
826.8	0.51675	5.1675	51.675	516.75	5167.5	51675
869.2	0.54325	5.4325	54.325	543.25	5432.5	54325
932.8	0.583	5.83	58.3	583	5830	58300
975.2	0.6095	6.095	60.95	609.5	6095	60950
1038.8	0.64925	6.4925	64.925	649.25	6492.5	64925
1081.2	0.67575	6.7575	67.575	675.75	6757.5	67575
1144.8	0.7155	7.155	71.55	715.5	7155	71550
1293.2	0.80825	8.0825	80.825	808.25	8082.5	80825
1356.8	0.848	8.48	84.8	848	8480	84800
1505.2	0.94075	9.4075	94.075	940.75	9407.5	94075
1568.8	0.9805	9.805	98.05	980.5	9805	98050
1717.2	1.07325	10.7325	107.325	1073.25	10732.5	107325
1780.8	1.113	11.13	111.3	1113	11130	111300
1929.2	1.20575	12.0575	120.575	1205.75	12057.5	120575
1992.8	1.2455	12.455	124.55	1245.5	12455	124550
2141.2	1.33825	13.3825	133.825	1338.25	13382.5	133825
2204.8	1.378	13.78	137.8	1378	13780	137800
2353.2	1.47075	14.7075	147.075	1470.75	14707.5	147075
2416.8	1.5105	15.105	151.05	1510.5	15105	151050
2565.2	1.60325	16.0325	160.325	1603.25	16032.5	160325
2628.8	1.643	16.43	164.3	1643	16430	164300
2777.2	1.73575	17.3575	173.575	1735.75	17357.5	173575
2840.8	1.7755	17.755	177.55	1775.5	17755	177550
2989.2	1.86825	18.6825	186.825	1868.25	18682.5	186825
3052.8	1.908	19.08	190.8	1908	19080	190800
3201.2	2.00075	20.0075	200.075	2000.75	20007.5	200075
3264.8	2.0405	20.405	204.05	2040.5	20405	204050
3413.2	2.13325	21.3325	213.325	2133.25	21332.5	213325

	Integrated counts					
IT (s)	***0.000625e/s***	***0.00625e/s***	***0.0625e/s***	***0.625e/s***	***6.25e/s***	***62.5e/s***
3476.8	2.173	21.73	217.3	2173	21730	217300
3625.2	2.26575	22.6575	226.575	2265.75	22657.5	226575
3688.8	2.3055	23.055	230.55	2305.5	23055	230550
3837.2	2.39825	23.9825	239.825	2398.25	23982.5	239825
3900.8	2.438	24.38	243.8	2438	24380	243800
4049.2	2.53075	25.3075	253.075	2530.75	25307.5	253075
4112.8	2.5705	25.705	257.05	2570.5	25705	257050

Table 6 Optimal readout pattern vs. photon flux. Red cell indicate saturation.

<table>
<tr><th>IT</th><th>0.000625e/s</th><th>0.00625e/s</th><th>0.0625e/s</th><th>0.625e/s</th><th>6.25e/s</th><th>62.5e/s</th></tr>
<tr><td>21.2</td><td colspan="6">RAPID-2</td></tr>
<tr><td>31.8</td><td colspan="6">RAPID-3</td></tr>
<tr><td>42.4</td><td colspan="6">RAPID-4</td></tr>
<tr><td>53</td><td>BRIGHT1-3</td><td colspan="5">RAPID-5</td></tr>
<tr><td>63.6</td><td colspan="6">RAPID-6</td></tr>
<tr><td>74.2</td><td>BRIGHT1-4</td><td colspan="5">RAPID-7</td></tr>
<tr><td>84.8</td><td>BRIGH2-3</td><td colspan="5">RAPID-8</td></tr>
<tr><td>95.4</td><td>BRIGHT1-5</td><td colspan="5">RAPID-9</td></tr>
<tr><td>106</td><td colspan="6">RAPID-10</td></tr>
<tr><td>116.6</td><td>BRIGHT1-6</td><td colspan="5">BRIGH2-4</td></tr>
<tr><td>127.2</td><td>MEDIUM2-2</td><td colspan="5">SHALLOW2-3</td></tr>
<tr><td>137.8</td><td colspan="6">BRIGHT1-7</td></tr>
<tr><td>148.4</td><td colspan="2" rowspan="2">BRIGH2-5</td><td colspan="4">SHALLOW4-3</td></tr>
<tr><td>159</td><td>BRIGHT1-8</td><td></td><td colspan="2">BRIGHT1-8</td></tr>
<tr><td>180.2</td><td colspan="2">SHALLOW2-4</td><td colspan="4">BRIGH2-6</td></tr>
<tr><td>190.8</td><td colspan="4">MEDIUM8-2</td><td colspan="2"></td></tr>
<tr><td>201.4</td><td>BRIGHT1-10</td><td colspan="5">SHALLOW4-4</td></tr>
<tr><td>212</td><td colspan="6">BRIGH2-7</td></tr>
<tr><td>233.2</td><td colspan="3"></td><td colspan="3">SHALLOW2-5</td></tr>
<tr><td>243.8</td><td colspan="5">BRIGH2-8</td><td></td></tr>
<tr><td>254.4</td><td colspan="6">SHALLOW4-5</td></tr>
<tr><td>275.6</td><td colspan="6">BRIGH2-9</td></tr>
<tr><td>286.2</td><td colspan="4"></td><td colspan="2">SHALLOW2-6</td></tr>
<tr><td>296.8</td><td rowspan="2">DEEP8-2</td><td colspan="4">MEDIUM8-3</td><td></td></tr>
<tr><td>307.4</td><td></td><td></td><td colspan="3">SHALLOW4-6</td></tr>
</table>

<table>
<tr><th>IT</th><th>0.000625e/s</th><th>0.00625e/s</th><th>0.0625e/s</th><th>0.625e/s</th><th>6.25e/s</th><th>62.5e/s</th></tr>
<tr><td>339.2</td><td colspan="2">MEDIUM2-4</td><td colspan="4">SHALLOW2-7</td></tr>
<tr><td>360.4</td><td colspan="5">SHALLOW4-7</td><td></td></tr>
<tr><td>392.2</td><td colspan="4"></td><td colspan="2" rowspan="2">SHALLOW2-8</td></tr>
<tr><td>402.8</td><td colspan="4">MEDIUM8-4</td></tr>
<tr><td>413.4</td><td colspan="6">SHALLOW4-8</td></tr>
<tr><td>445.2</td><td colspan="4"></td><td colspan="2">SHALLOW2-9</td></tr>
<tr><td>466.4</td><td colspan="5">SHALLOW4-9</td><td></td></tr>
<tr><td>498.2</td><td colspan="4"></td><td colspan="2">SHALLOW2-10</td></tr>
<tr><td>508.8</td><td colspan="3">DEEP8-3</td><td colspan="3">MEDIUM8-5</td></tr>
<tr><td>519.4</td><td colspan="4" rowspan="2">SHALLOW4-10</td><td colspan="2"></td></tr>
<tr><td>551.2</td><td colspan="2">MEDIUM2-6</td></tr>
<tr><td>614.8</td><td colspan="4" rowspan="2">MEDIUM8-6</td><td colspan="2">MEDIUM8-6</td></tr>
<tr><td>657.2</td><td colspan="2">MEDIUM2-7</td></tr>
<tr><td>720.8</td><td colspan="3" rowspan="2">DEEP8-4</td><td colspan="3">MEDIUM8-7</td></tr>
<tr><td>763.2</td><td></td><td colspan="2">MEDIUM2-8</td></tr>
<tr><td>826.8</td><td colspan="6">MEDIUM8-8</td></tr>
<tr><td>869.2</td><td colspan="4"></td><td colspan="2">MEDIUM2-9</td></tr>
<tr><td>932.8</td><td colspan="3" rowspan="2">DEEP8-5</td><td colspan="3">MEDIUM8-9</td></tr>
<tr><td>975.2</td><td></td><td colspan="2">MEDIUM2 MEDIUM2</td></tr>
<tr><td>1038.8</td><td colspan="6">MEDIUM8-10</td></tr>
<tr><td>1081.2</td><td colspan="4"></td><td colspan="2">DEEP2-6</td></tr>
<tr><td>1144.8</td><td colspan="6">DEEP8-6</td></tr>
<tr><td>1293.2</td><td colspan="3"></td><td colspan="3">DEEP2-7</td></tr>
<tr><td>1356.8</td><td colspan="6">DEEP8-7</td></tr>
<tr><td>1505.2</td><td colspan="3"></td><td colspan="3">DEEP2-8</td></tr>
<tr><td>1568.8</td><td colspan="6">DEEP8-8</td></tr>
<tr><td>1717.2</td><td colspan="3"></td><td colspan="2">DEEP2-9</td><td></td></tr>
<tr><td>1780.8</td><td colspan="5">DEEP8-9</td><td></td></tr>
<tr><td>1929.2</td><td colspan="3"></td><td colspan="2">DEEP2-10</td><td></td></tr>
<tr><td>1992.8</td><td colspan="5">DEEP8-10</td><td></td></tr>
<tr><td>2141.2</td><td colspan="3"></td><td colspan="2">DEEP2-11</td><td></td></tr>
<tr><td>2204.8</td><td colspan="5">DEEP8-11</td><td></td></tr>
<tr><td>2353.2</td><td colspan="3"></td><td colspan="2">DEEP2-12</td><td></td></tr>
<tr><td>2416.8</td><td colspan="5">DEEP8-12</td><td></td></tr>
<tr><td>2565.2</td><td colspan="3"></td><td colspan="2">DEEP2-13</td><td></td></tr>
<tr><td>2628.8</td><td colspan="5">DEEP8-13</td><td></td></tr>
<tr><td>2777.2</td><td colspan="3"></td><td colspan="2">DEEP2-14</td><td></td></tr>
<tr><td>2840.8</td><td colspan="5">DEEP8-14</td><td></td></tr>
</table>

IT	0.000625e/s	0.00625e/s	0.0625e/s	0.625e/s	6.25e/s	62.5e/s
2989.2				DEEP2-15		🟥
3052.8	DEEP8-15					🟥
3201.2				DEEP2-16		🟥
3264.8	DEEP8-16					🟥
3413.2				DEEP2-17		🟥
3476.8	DEEP8-17					🟥
3625.2				DEEP2-18		🟥
3688.8	DEEP8-18					🟥
3837.2				DEEP2-19		🟥
3900.8	DEEP8-19					🟥
4049.2				DEEP2-20		🟥
4112.8	DEEP8-20					🟥

6.0 Summary of the optimal readout patterns

In paper 1 I have shown that in readout noise limited regime only 47 readout patterns are optimal. Table 7 summarizes the situation when one takes into account the photon flux. Of the original 110 readout patterns, 21 are not optimal: 9 because they correspond to *n*=1; the remaining 12 are eliminated because they correspond to a degenerate integration time for which some another mode always provides higher signal-to-noise, regardless on the photon flux.

We are still left with 89 "optimal" readout modes, which represents a substantial increase with respect to the 47 only required by the readout-noise limited case discussed in Paper 1.

Table 7 Summary table listing the optimal readout patterns

n	RAPID	BRIGHT1	BRIGHT2	SHALLOW2	SHALLOW4	MEDIUM2	MEDIUM8	DEEP2	DEEP8
1	🟥	🟥	🟥	🟥	🟥	🟥	🟥	🟥	🟥
2	RAPID-2	🟥	🟥	SHALLOW2	🟥	MEDIUM2-2	MEDIUM8-2	🟥	DEEP8-2
3	RAPID-3	BRIGHT1-3	BRIGH2-3	SHALLOW2-3	SHALLOW4-3	🟥	MEDIUM8-3	🟥	DEEP8-3
4	RAPID-4	BRIGHT1-4	BRIGH2-4	SHALLOW2-4	SHALLOW4-4	MEDIUM2-4	MEDIUM8-4	🟥	DEEP8-4
5	RAPID-5	BRIGHT1-5	BRIGH2-5	SHALLOW2-5	SHALLOW4-5	🟥	MEDIUM8-5	🟥	DEEP8-5
6	RAPID-6	BRIGHT1-6	BRIGH2-6	SHALLOW2-6	SHALLOW4-6	MEDIUM2-6	MEDIUM8-6	DEEP2-6	DEEP8-6
7	RAPID-7	BRIGHT1-7	BRIGH2-7	SHALLOW2-8	SHALLOW4-7	MEDIUM2-7	MEDIUM8-7	DEEP2-7	DEEP8-7
8	RAPID-8	BRIGHT1-8	BRIGH2-8	🟥	SHALLOW4-8	MEDIUM2-8	MEDIUM8-8	DEEP2-8	DEEP8-8
9	RAPID-9	🟥	BRIGH2-9	SHALLOW2-9	SHALLOW4-9	MEDIUM2-9	MEDIUM8-9	DEEP2-9	DEEP8-9
10	RAPID-10	BRIGHT1-10	🟥	SHALLOW2-10	SHALLOW4-10	MEDIUM2-10	MEDIUM8-10	DEEP2-10	DEEP8-10

n	RAPID	BRIGHT1	BRIGHT2	SHALLOW2	SHALLOW4	MEDIUM2	MEDIUM8	DEEP2	DEEP8
11								DEEP2-11	DEEP8-11
12								DEEP2-12	DEEP8-12
13								DEEP2-13	DEEP8-13
14								DEEP2-14	DEEP8-14
15								DEEP2-15	DEEP8-15
16								DEEP2-16	DEEP8-16
17								DEEP2-17	DEEP8-17
18								DEEP2-18	DEEP8-18
19								DEEP2-19	DEEP8-19
20								DEEP2-20	DEEP8-20

7.0 Conclusions

NIRCAM readout strategy allows for 110 readout patterns, i.e. combinations of readout samples and number of groups. They correspond to 75 unique integration times with at least 2 reads. Some of the integration times are degenerate, allowing for multiple choices of readout patterns. In this report I have shown how the optimal choice of readout pattern depends on the flux incident on a pixel. I provide tables that list a) the best readout pattern for every integration times over a wide range of photon fluxes; b) how the signal to noise (relative to the maximum theoretically achievable with the longest readout pattern in the absence of cosmic rays) scales with the photon flux for each optimal readout pattern; c) the integrated photons corresponding to each optimal readout pattern; d) a summary “map” of the optimal readout pattern vs. exposure time and photon flux.

The ultimate goal of this analysis is to optimize the strategy for NIRCam observations. Our final step will require taking into account that the signal to noise associated to a point source results from all pixels composing the source PSF, as they receive different amount of illumination and therefore would ideally require individual optimal readout mode. The methods used in this report set the basis for finding the readout pattern that provides the best compromise, i.e. the highest signal to noise, taking into account the source and sky brightness and integration time. This analysis will be the subject of a future report.

8.0 References

M. Rieke, 2005 “NIRCAM Sensitivity Calculations”, JWST-CALC-003894

M. Robberto, 2009a “NIRCAM Optimal Readout Modes”, JWST-STScI-001721, SM-12 (Paper 1)

M. Robberto, 2009b “Derivation of the correct noise equation for general MULTIACCUM readout”, JWST-STScI-001853, SM-12 (Paper 2)